



# Simulation of methane/air non-premixed turbulent flames based on REDIM simplified chemistry

Felipe Minuzzi<sup>1</sup>  · Chunkan Yu<sup>2</sup> · Ulrich Maas<sup>2</sup>

Received: 13 February 2019 / Accepted: 5 August 2019 / Published online: 10 October 2019  
© Springer Nature B.V. 2019

## Abstract

Combustion simulations involve the modeling of chemical kinetics, and due to the complexity of detailed mechanisms, chemistry reduction techniques are necessary. One model reduction strategy is the reaction-diffusion manifold (REDIM) method, and to obtain the REDIM, an evolution equation must be solved till its stationary solution and a gradient estimation is needed, provided e.g. from flamelet solutions with detailed chemistry. In this work, the REDIM technique is applied to simulate methane/air turbulent flames based on a simplified gradient estimation. This strategy uses less information in constructing the REDIM, increasing computational efficiency while reducing computational costs. Validation is performed for non-premixed laminar flames. A RANS/transported-PDF framework for the simulation of turbulent reacting flows is presented and used to validate the proposed model. Results show that the simplified gradient estimation is enough to simulate turbulent flames at moderate Reynolds number, which demonstrates the suitability of REDIM as reduced kinetic model in reactive flows.

**Keywords** Chemical reduction · REDIM · RANS · Turbulent flame · Methane

## 1 Introduction

The simulation of reactive flows involves a complex modeling of the interaction of thermodynamics, chemical kinetics, molecular transport and fluid dynamics. Combustion is a

---

✉ Felipe Minuzzi  
felipe.minuzzi@ufrgs.br

Chunkan Yu  
chunkan.yu@kit.edu

Ulrich Maas  
ulrich.maas@kit.edu

<sup>1</sup> Grupo de Mecânica dos Fluidos Reativos, Instituto Nacional de Pesquisas Espaciais - INPE, Rod. Presidente Dutra, km 40, 12630-000, Cachoeira Paulista, SP, Brazil

<sup>2</sup> Institute of Technical Thermodynamics, Karlsruhe Institute of Technology - KIT, Engelbert-Arnold-Str. 4, 76131, Karlsruhe, Germany

process that releases heat and may generate instabilities in the flow due to fluctuations and gas expansion, which cause a transition to turbulence [1]. In most cases, in practical devices, combustion occurs under turbulent flow conditions [2], and the understanding of the underlying processes is crucial for the physical description of the phenomenon. Turbulence models are based on the Navier-Stokes equations and closures hypothesis, which are based on dimensional arguments and empirical data [3].

Numerical simulation of turbulent flows can be organized in three groups [1]: DNS, LES and RANS. Direct numerical simulation (DNS) is a technique where the Navier-Stokes equations are fully resolved without modeling, that is, all relevant scales are solved. However, its computational cost increases rapidly with increasing Reynolds number, so its applicability is restricted to low to moderate Reynolds numbers [4, 5]. Large eddy simulation (LES) [4, 6–8] resolves explicitly the large scales of the flow, while the smallest are modeled by subgrid models. Reynolds averaged Navier-Stokes (RANS) is a technique with acceptable computational cost in which the balance equations are averaged, and closure models are used to deal with the turbulence [6].

The interaction between turbulence and chemistry is a well known challenge in numerical simulations and high order methods with small time steps ought to be used. The modeling of the chemical source term is a difficult task [9], since they are influenced by turbulent mixing, molecular transport and chemical kinetics [7]. Infinitely fast chemistry is a simple assumption to overcome this problem [3], but then complicated reacting flows with ignition, extinction and pollutant formation cannot be predicted.

The probability density function (PDF) is a model that can overcome the complexity of solving the reaction source term in turbulent flows. In a transported-PDF equation, chemical source term is in a closed form, avoiding any modeling [10, 11]. Furthermore, the PDF of velocity and thermo-kinetics scalars and their averages and statistical moments can be obtained.

Modeling of combustion is a complex phenomenon, since the fuel oxidation mechanisms can have thousands of elementary reactions and hundreds or thousands of chemical species. Turbulence can also enhance the complexity and dimension of the system. Therefore, using detailed kinetic mechanisms is in most cases computationally prohibitive, and techniques for chemical reduction are necessary in order to develop reduced models with less variables and moderate stiffness [12], while maintaining the accuracy and comprehensiveness of the detailed model.

There are two main categories of reduction techniques for kinetic mechanisms: time scale analysis and the generation of skeletal mechanisms [13]. The latter consists in identifying the important and necessary species and in generating the mechanism only with those. Some examples are the directed relation graph (DRG) [14] and directed relation graph with error propagation (DRGEP) [15] and sensitivity analysis based on Jacobian analysis [12]. Time scale analysis is used primarily to identify a gap between fast and slow time scales in species trajectory on the composition state space and use this to describe the system dynamics. Examples are the Quasi-Steady-State Assumption (QSSA) [16] and Partial Equilibrium (PE), Intrinsic Low-Dimensional Manifolds (ILDM) [17], Flame Prologation of ILDM (FPI) [18], Computational Singular Perturbation (CSP) [19], Flamelet approach [20] and its developments, as Flamelet with Progress Variable [21] and Flamelet Generated Manifolds (FGM) [22]. A complete review of reduction methods can be found in [23–26].

This difference in time scales in chemical systems yields the existence of low-dimensional manifolds imbedded in the state space that can be used to describe the full dynamics of the model [17]. These manifolds have the property of attracting the trajectories

of species concentrations and maintain close to it for all times [17]. The reaction-diffusion manifold (REDIM) [27] has the advantage of taking into account physical transport processes when generating the manifold.

To obtain the REDIM, an evolution equation must be solved till its stationary solution and a gradient estimation is needed. This estimation is based on numerical simulations with detailed mechanisms. One strategy is to take flamelets with different strain rates, to cover the domain from stable flames until the extinction limit. As explained by Bykov et al. [28], the flamelet approach used for the initial guess represents a stationary solution set of detailed systems that are theoretically close to the REDIM for specific estimates of the gradient. To cover the domain where the flamelets do not exist, non-stationary flamelets (extinguishing) flames are chosen. The lower boundary will be a mixture line, i.e., a linear trajectory that describes pure mixing in the state space. An algorithm for solving the REDIM equations is presented in [29].

The REDIM method has already been used extensively in literature for different combustion scenarios simulations. Fischer et al. [30] used PDF simulations to analyse the ignition of free turbulent jets of propane, ethylene and hydrogen, while in the works of Wang et al. [31, 32], large eddy simulation with filtered density functions were used with REDIM to simulate turbulent flames. Recently, flame-wall interactions that perturb the system states by heat loss and catalytic reactions was analysed in the context of REDIM [33]. Multi-directional molecular diffusion was also studied in terms of the REDIM [34]. A coupled strategy between REDIM and the Progress Variable Method was developed by Benzinger et al. [35], based on a new variable: the normalized strength of molecular transport. In [28], the instationary behaviour of counterflow non-premixed flames with REDIM is studied and the ability of REDIM to describe transient processes of extinction and re-ignition.

The purpose of the present work is to show that a simplified gradient estimation used to generate the REDIM is sufficient to obtain accurate results in the simulations. The advantage of this framework is that allows to use less information about the full model and to decrease computational costs. The model is validated in a methane/air non-premixed counterflow laminar flame and used for simulation of two piloted turbulent jet flames, with low and moderate degree of local extinction, using a hybrid RANS/transported-PDF model.

## 2 Reduction of Chemical Kinetics: REDIM

The thermochemical state in a reactive system with  $n_{sp}$  species can be described by the  $n = n_{sp} + 2$  dimension vector  $\Psi = (h, p, \phi_1, \dots, \phi_{n_{sp}})^T$ , where  $h$  is the specific enthalpy,  $p$  the pressure and  $\phi_i$  is the specific mole fraction of species  $i$ , defined as  $\phi_i = x_i/M_{\text{mean}}$  ( $x_i$  is the molar fraction and  $M_{\text{mean}}$  the mean molar mass). The thermochemical state changes due to chemical and transport processes according to the partial differential equation system [27]

$$\frac{\partial \Psi}{\partial t} = \mathbf{F}(\Psi) - \mathbf{u} \cdot \text{grad}(\Psi) - \frac{1}{\rho} \text{div} [\mathbf{D} \cdot \text{grad}(\Psi)] = \Phi(\Psi) \quad (1)$$

Here,  $\mathbf{u}$  is the velocity,  $\mathbf{D}$  is the  $n \times n$ -dimension transport matrix,  $\mathbf{F}$  is the  $n$ -dimensional source term that accounts for the chemical reactions and  $\rho$  the density.

The difference of fast and slow time scales in chemical systems yields the existence of low-dimensional manifolds imbedded in the state space that can be used to describe the full dynamics of the model [17]. After the fast time scales are exhausted, the system

dynamics is governed by the  $m_s$  slowest modes ( $m_s \ll n$ ), i.e., the system solution is within a  $m_s$ -dimensional manifold in the state space. This manifold  $\mathcal{M}$  is defined as

$$\mathcal{M} = \{ \Psi : \Psi = \Psi(\theta), \Psi : R^{m_s} \rightarrow R^n \}, \tag{2}$$

where  $\theta$  is the vector of local coordinates, i.e., the  $m_s$ -dimensional vector that parametrizes the manifold.

To obtain the manifold, an invariance condition is applied. This condition implies that, after the states approached the manifold (fast time scales vanish), they will evolve within or close to this surface, for all times. As a consequence, for all  $\Psi \in \mathcal{M}$ , it holds that  $\Phi(\Psi) \in T_\Psi \mathcal{M}$ , i.e., the vector field  $\Phi$  (the right-hand-side of Eq. 1) applied to the vectors of the manifold belongs to the tangent space of  $\mathcal{M}$ .

Since  $\Phi(\Psi)$  belongs to the tangent space of the manifold, it is orthogonal to the normal space of  $\mathcal{M}$ ,

$$(\Psi_\theta^\perp(\theta))^T \cdot \Phi(\Psi) = 0, \tag{3}$$

for all  $\theta$ , where  $\Psi_\theta^\perp$  represents the normal space of  $\mathcal{M}$ . Therefore, the projection of  $\Phi$  in the normal space of  $\mathcal{M}$  is also orthogonal to the field. We define the projection operator as

$$P_{(T\mathcal{M})^\perp} [\Phi(\Psi)] = \left( \Psi_\theta^\perp(\theta) \cdot \Psi_\theta^+(\theta) \right) \cdot \Phi(\Psi) \tag{4}$$

where  $\Psi_\theta^+$  is the Moore-Penrose pseudo-inverse matrix. This matrix always exists, provided that the columns of  $\Psi_\theta$  are linearly independent. Nevertheless, this condition can always be obtained through a suitable choice of the local coordinates  $\theta$ . Since

$$P_{(T\mathcal{M})^\perp} [\Phi(\Psi)] \cdot \Phi(\Psi) = \left( I - \Psi_\theta(\theta) \cdot \Psi_\theta^+(\theta) \right) \cdot \Phi(\Psi(\theta)), \tag{5}$$

we can conclude that

$$\left( I - \Psi_\theta \Psi_\theta^+ \right) \cdot \Phi(\Psi) = 0 \tag{6}$$

where  $\Psi_\theta$  is the Jacobian of  $\Psi$  with respect to  $\theta$ . To integrate Eq. 6, the strategy is to rewrite the equation as a system of parabolic partial differential equations [27], given by

$$\frac{\partial \Psi(\theta)}{\partial t} = \left( I - \Psi_\theta(\theta) \cdot \Psi_\theta^+(\theta) \right) \cdot \left\{ \mathbf{F}(\Psi(\theta)) - \frac{1}{\rho} \left[ (\mathbf{D}\Psi_\theta \cdot \chi(\theta))_\theta \cdot \chi(\theta) \right] \right\}. \tag{7}$$

where  $\chi(\theta) = \text{grad}(\theta)$  is a gradient estimation. Then, an invariant  $m_s$ - dimensional slow manifold, referred to as Reaction Diffusion Manifold (REDIM), can be obtained through the stationary solution  $\Psi(\theta, \infty)$  of Eq. 7. To integrate this equation until it converges, it is necessary to define the gradient  $\chi(\theta)$  for the starting manifold.

To obtain the gradient estimation, one strategy would be to take the flamelets based on detailed chemistry with different strain rates (a, unity: 1/s). As explained in [28], this would represent a stationary solution set of detailed systems that are theoretically close to the REDIM for specific estimates of the gradient. To cover the domain where stationary flamelets do not exist, unsteady flamelets (extinguishing) flames are chosen.

In the present work, the gradient estimation consists of a stable flamelet solution with low strain rate and a pure mixing line as boundaries, and one flamelet solution with an intermediate strain rate as initial condition. More details will be shown in Section 5.1.

### 3 Hybrid RANS/Transported-PDF Model

In the RANS model, the favre-averaged conservation equations for mass and momentum are solved [4]. The conservation equations for energy needs not to be solved, since the favre averaged temperature  $\tilde{T}$  is determined in the PDF part from the thermo-kinetic state of the fluid. Consequently, the averaged ideal gas law ( $\bar{p} = \bar{\rho} \tilde{R}_g \tilde{T}$ ) together with conservation equations, are solved simultaneously to obtain the mean velocities. The unclosed term of Reynolds stresses  $\overline{\rho u_i'' u_j''}$  is obtained from the PDF part [36].

A joint PDF (JPDF) of velocity, composition and turbulent frequency  $f_{\omega \mathbf{U} \Phi}(\Theta, \mathbf{V}, \Psi; \mathbf{x}, t)$  is employed [37]. This is a one-point, one-time joint PDF which has the main advantage to treat chemical reaction exact without any modeling assumptions.

A transported-PDF equation is solved to obtain the PDF of velocity [36], which overcomes the problem that generally the PDF of a flow is a priori unknown [10, 11]. The transported-PDF equation for  $f_{\omega \mathbf{U} \Phi}(\Theta, \mathbf{V}, \Psi; \mathbf{x}, t)$  is given by [4]

$$\begin{aligned} \rho(\Psi) \frac{\partial f}{\partial t} + \rho(\Psi) V_i \frac{\partial f}{\partial x_i} - \frac{\partial \bar{p}}{\partial x_i} \frac{\partial f}{\partial V_i} + \frac{\partial \rho(\Psi) S_\alpha(\Psi)}{\partial \Psi_\alpha} \\ = - \frac{\partial}{\partial V_i} \left( \overline{\frac{\partial \tau'_{ij}}{\partial x_j} - \frac{\partial p'}{\partial x_l} \Big|_{\Theta, \mathbf{V}, \Psi}} \right) \cdot f + \frac{\partial}{\partial \Psi_\alpha} \left( \overline{\frac{\partial J'_{\alpha,l}}{\partial x_l} \Big|_{\Theta, \mathbf{V}, \Psi}} \right) \cdot f \\ - \frac{\partial}{\partial \theta} \left( \overline{\frac{D\omega}{Dt} \Big|_{\Theta, \mathbf{V}, \Psi}} \right) \cdot f, \end{aligned} \tag{8}$$

where  $\mathbf{x}$  is the spatial position and  $t$  the time,  $p'$  is the pressure fluctuation,  $\Theta, \mathbf{V}$  and  $\Psi$  are the sample space variables of the turbulent frequency  $\omega$ , velocity  $\mathbf{U}$  and composition  $\Phi$ , respectively.  $S_\alpha(\Psi)$  denotes the chemical source term,  $D/Dt$  denotes the material derivative,  $\bar{\tau}_{ij}$  the mean viscous stress,  $p$  the mean pressure,  $\rho$  the density and  $J_\alpha$  the diffusion flux.

In Eq. 8 the mean viscous stress  $\bar{\tau}_{ij}$  and the mean diffusion flux  $\bar{J}_\alpha$  are neglected because both terms are of little importance for flows with high Reynolds numbers [4]. It can be observed that all terms on the left-hand side are in closed form, including the chemical source term. However, all the conditional terms on the right-hand side are unclosed and must be modelled [10, 11, 38].

The numerical integration of the transported-PDF equation is solved using a particle method [36]. The particle location is evolved according to the particle velocity (superscript \* indicates particle quantity) through  $dx_i^* = \mathbf{U} dt$ , where  $\mathbf{U}$  is the total velocity, given by the sum of the averaged velocity  $\tilde{u}$  and a fluctuation  $u^*$ . In our hybrid approach, the averaged velocity is obtained via the RANS method and the fluctuation by the transported-PDF equation (see Fig. 1).

The velocity fluctuation is represented by stochastic particle  $u_i^*$ , which is modeled by the simplified Langevin model (SLM) [4], given by

$$\frac{du_i^*}{dt} = \frac{1}{\langle \rho \rangle} \frac{\partial \langle \rho \rangle \widetilde{u_i^* u_j^*}}{\partial x_j} - u_j^* \frac{\partial \tilde{u}_i}{\partial x_j} - \left( \frac{1}{2} + \frac{3}{4} C_0 \right) \Omega u_i^* + (C_0 \Omega k)^{1/2} \tag{9}$$

where  $\Omega$  is the conditional turbulence frequency, related to the model constant  $C_\Omega$  through [38]

$$\Omega = C_\Omega \frac{\langle \rho^* \omega^* | \omega^* \geq \tilde{\omega} \rangle}{\langle \rho \rangle} \tag{10}$$

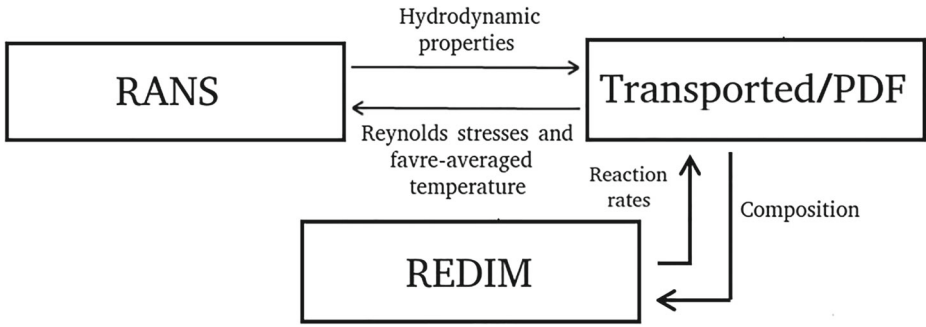


**Fig. 1** Overview of the algorithm coupling the RANS/transported-PDF to the REDIM reduction method

in which  $\tilde{\omega}$  is the averaged turbulent frequency,  $k$  is the turbulent kinetic energy ( $k = \widetilde{u_i u_i} / 2$ ) and  $\langle \rho \rangle$  the averaged density.

The particle turbulence frequency  $\omega^*$  is modeled based on the gamma-distribution model [4], and reads

$$\frac{d\omega^*}{dt} = -C_3(\omega^* - \tilde{\omega})\Omega - \Omega\omega^* \left[ C_{\omega 2} - \frac{C_{\omega 1}}{k\Omega} \left( -\widetilde{u_i u_j} \frac{\partial \tilde{u}_i}{\partial x_j} \right) \right] + (2C_3 C_4 \tilde{\omega} \Omega \omega^*)^{1/2}. \quad (11)$$

Coefficients  $C_\Omega$ ,  $C_{\omega 1}$ ,  $C_{\omega 2}$ ,  $C_0$ ,  $C_3$  and  $C_4$  in Eqs. 9 and 11 will be given in Table 1.

The evolution of the composition vector can be calculated as

$$\frac{d\Phi^{*,i}}{dt} = \mathbf{S}(\Phi^{*,i}) + \mathbf{M}, \quad i = 1, 2, \dots, N_p, \quad (12)$$

in which  $N_p$  is the number of particles per cell.  $\mathbf{S}(\Phi^{*,i})$  is the source term and  $\mathbf{M}$  is the effect of molecular mixing process [10, 11]. The source term, as already mentioned, appears in exact form in the PDF framework, but the mixing process is modeled by a mixing model. We choose to model the mixing process using the modified Curl’s model (MCM) [39]. In MCM, pairs of particles within the same cell are randomly selected and mixed with some intensity [40] and the rate of mixing is determined by the coefficient  $C_\phi$ .

**Table 1** Parameters used in the simulation of the turbulent flame

Turbulence frequency model	
$C_\Omega$	0.6893
$C_{\omega 1}$	0.7
$C_{\omega 2}$	0.9
$C_3$	1.0
$C_4$	1.25
Simplified langevin model	
$C_0$	2.1
Mixing model	
$C_\phi$	3.6

Based on Eqs. 9, 11 and 12, the transported-PDF equation for the joint PDF  $f_{\omega\mathbf{U}\Phi}$  is given by [10, 37]

$$\begin{aligned} & \frac{\partial \langle \rho \rangle f}{\partial t} + \frac{\partial \langle \rho \rangle f(\tilde{u}_j + u''_j)}{\partial x_j} - \frac{\partial \tilde{u}_i}{\partial x_j} \frac{\partial (\langle \rho \rangle f) u''_j}{\partial u''_i} + \frac{1}{\langle \rho \rangle} \frac{\partial \langle \rho \rangle \widetilde{u''_i u''_j}}{\partial x_j} \frac{\partial \langle \rho \rangle f}{\partial u''_i} \\ &= \left( \frac{1}{2} + \frac{3}{4} C_0 \right) \Omega \frac{\partial \langle \rho \rangle f u''_i}{\partial u''_i} + \frac{1}{2} (C_0 \epsilon) \frac{\partial^2 \langle \rho \rangle f}{\partial (u''_i)^2} \\ &+ \frac{\partial \langle \rho \rangle f \Omega C_3 (\theta - \tilde{\omega})}{\partial \theta} + \frac{\partial}{\partial \theta} \left( \langle \rho \rangle f \left[ C_{\omega 2} - \frac{C_{\omega 1}}{k \Omega} \left( -\widetilde{u''_i u''_j} \frac{\partial \tilde{U}_i}{\partial x_j} \right) \right] \Omega \theta \right) \\ &+ C_3 C_4 \tilde{\omega} \Omega \frac{\partial^2 \theta \langle \rho \rangle f}{\partial \theta^2} - \frac{\partial}{\partial \Psi_\alpha} [\langle \rho \rangle f (S_\alpha(\Psi) + M_\alpha)]. \end{aligned} \tag{13}$$

The hybrid RANS/Transported-PDF method provides the advantage of using fewer particles per cell compared to traditional particle methods, decreasing computational time [38]. To improve efficiency, particle number control strategy is applied, and a constant number of particles per grid cell, whether it is large or small cells, is desired. The maximum number of particles within one grid cell is  $1.2 \times N_p$ , whereas the minimum number is  $0.8 \times N_p$ . If the particle number is less than the minimum number, the particles are cloned until a target value (here  $0.8 \times N_p$  particles/cell) is reached. The particles will be eliminated through the statistical elimination algorithm: the two lightest particles in a cell are considered, and one of them is deleted, using a probability based on particles weights [41].

The coupling between the RANS/transported-PDF model and the REDIM is shown in Fig. 1. Equation 12 is solved using the reduced chemical kinetics of particles  $\phi^*$  and the source terms  $\mathbf{S}(\Phi^{*,i})$  are calculated from a lookup table generated based on REDIM method. The Reynolds stresses  $\overline{\rho u''_i u''_j}$  and the favre-averaged temperature  $R_g \tilde{T}$  are calculated through the particle method, and then used to solve the favre-averaged conservation equations of mass and momentum. The RANS provides the hydrodynamic properties, such as the mean velocity, which is used in the particle method to obtain the particle position, velocity and turbulent frequency.

By solving only the fluctuations of the velocities in the PDF part we avoid the drawback of duplicate scalar fields [38, 42], where some quantities are calculated both by the RANS and the PDF approach. To obtain convergence of the simulation, one needs consistent values i.e., this twice determined scalars should yields similar results. The level of consistency depends mainly on the equivalence of the turbulence models used in both methods [42]. Nevertheless, in our numerical algorithm, we do not have duplicate scalar fields.

### 4 Numerical Configuration

The methane/air piloted turbulent jet Sandia flame [43, 44] is used as experimental test-case to simulate the turbulent flame. We consider Flames D and E, since the first shows a small and the latter a moderate degree of local extinction, which allows a useful comparison for the reduced model presented in this work. Both flames consist of a main fuel jet with  $D = 7.2\text{mm}$  diameter, with a mixture composition of 25% methane and 75% dry air by volume. The initial temperature is 294K.

The coaxial pilot has an inner diameter of 7.7mm and an outer diameter of 18.2mm, with a mixture of  $C_2H_2$ , air,  $CO_2$  and  $N_2$ , and is operated at lean condition ( $\phi = 0.77$ ), with the same nominal enthalpy and equilibrium composition as methane/air at this equivalence ratio. The energy release of the pilot is approximately 6% of the main jet for each flame. The piloted burner is fixed with the jet exit approximately 15cm above the wind tunnel exit, which has a dimension of 30cm  $\times$  30cm. Figure 2 presents a sketch of the flame configuration used in the simulations.

For the Sandia flame D, the Reynolds number of the jet is 22400, which represents a jet velocity of 49.6m/s, and for the Sandia flame E, the Reynolds number of the jet is 33600, yielding a jet velocity of 74.4m/s. The experimental data are measured with spontaneous Raman and Rayleigh scattering for major species and temperature, and LIF is used for the concentrations of OH and NO. The uncertainties of the measurements are estimated to be within  $\pm 2\%$  for mass fractions of  $N_2$ ,  $O_2$ ,  $CH_4$ ,  $CO_2$ ,  $H_2O$ ,  $H_2$  and temperature,  $\pm 5\%$  for OH and CO, and  $\pm 10\%$  for NO [44].

#### 4.1 Simulation of the turbulent flame

The CFD code SPARC [45] is used for the simulation of the flow field. It is based on a finite volume method that solves the RANS equations on block structured domains. A cylindrical system is employed, with  $x$  denoting the downstream and  $r$  the radial coordinates.

The transported-PDF equation is solved by using a Monte-Carlo particle method [36], where a set of stochastic differential equations is solved to the evolution of particles. As already mentioned, the evolution of velocity is modeled by the simplified Langevin model (SLM) [4], the turbulent frequency is based on the gamma-distribution model [4] and the mixing model is modeled by the modified Curl's model (MCM) [39]. We adopt  $C_\phi = 3.6$ , which is required to obtain the burning index, consistent with the range of 3.3–3.8 proposed by Cao et al. [40] for Sandia flames D and E.

The simulation is performed for a  $120D \times 40D$  domain discretized by  $51 \times 42$  cells (total of 2142 cells), and the initial number of particle per cell is  $N_p = 50$ . In this work, radiation is not considered. Table 1 lists the parameters and their respective values for each model used in the simulation.

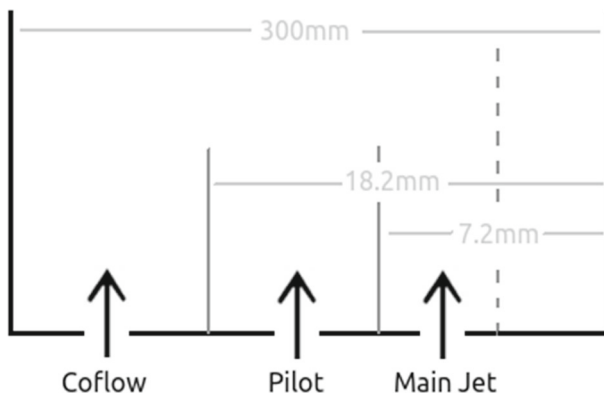


Fig. 2 Schematic Sandia flame configuration



## 5 Results and Discussion

### 5.1 Implementation of chemistry reduction with REDIM

To validate the REDIM method for the relevant mixture compositions, simulations of a counterflow non-premixed flame are performed. This configuration of flame consists in two opposed ducts, where the laminar flow of fuel leaves one duct and stagnates against the laminar flow of oxidant emerging from the other side [5]. The composition of both streams are the same as Sandia flame [43, 44], that is, 25% methane and 75% air at the fuel side, with initial temperature of 294K, while the oxidant size is pure air (79%  $N_2$  and 21%  $O_2$ ), with initial temperature of 291K. The distance of the ducts is 8cm and the calculations are performed for 1atm.

The initial guess consists of a manifold estimation and the boundary conditions of the REDIM. In this work, we consider a simplified configuration of the initial guess, formed by one stable flamelet solution with high stretch rate and a pure mixing line (extinguished flame) as boundaries, and one flamelet solution with a low stretch rate. The initial guess is allowed to evolve according to (7), until the REDIM is obtained as the steady-state solution. For the estimation of the gradient  $\chi(\theta)$  in (7), we have used only one single flamelet solution, namely, the one for low stretch rate (see Fig. 3). All these profiles were calculated using the code INSFLA [46] and GRI 3.0 as the detailed mechanism [47]. For simplification, a unity Lewis number is considered. Figure 3 shows the initial guess (a) and the projection of REDIM onto the  $N_2$  -  $CO_2$  -  $OH$  composition space (b).

The progress variables used are the specific mole fractions of  $CO_2$  ( $\phi_{CO_2}$ ) and  $N_2$  ( $\phi_{N_2}$ ), where the first represents the reaction and the second the mixing. In the REDIM, all the thermo-chemical quantities such as enthalpy, mixture fraction and mass fractions of species are functions of  $\phi_{CO_2}$  and  $\phi_{N_2}$ .

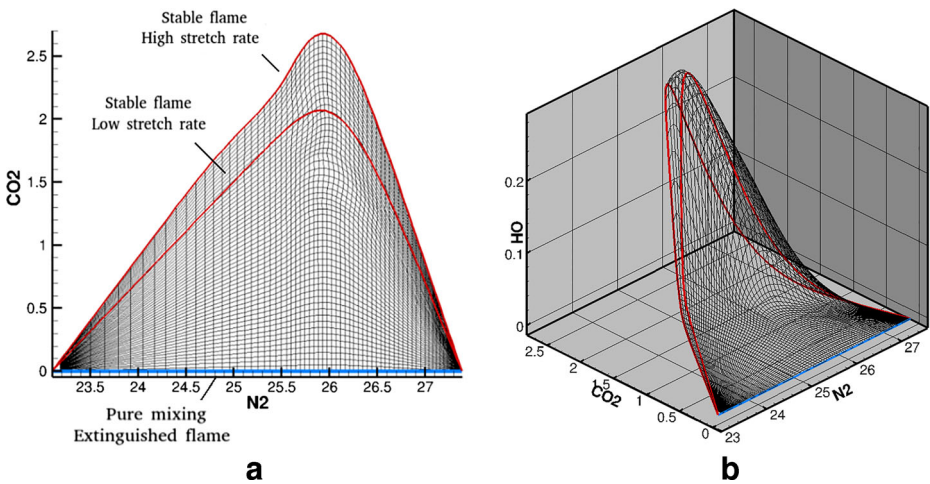


**Fig. 3** Initial profile (a) and (b) the projection of REDIM onto the  $N_2$  -  $CO_2$  -  $OH$  composition space. Red lines represent stable stationary flamelets solution and blue line represent a pure mixing profile

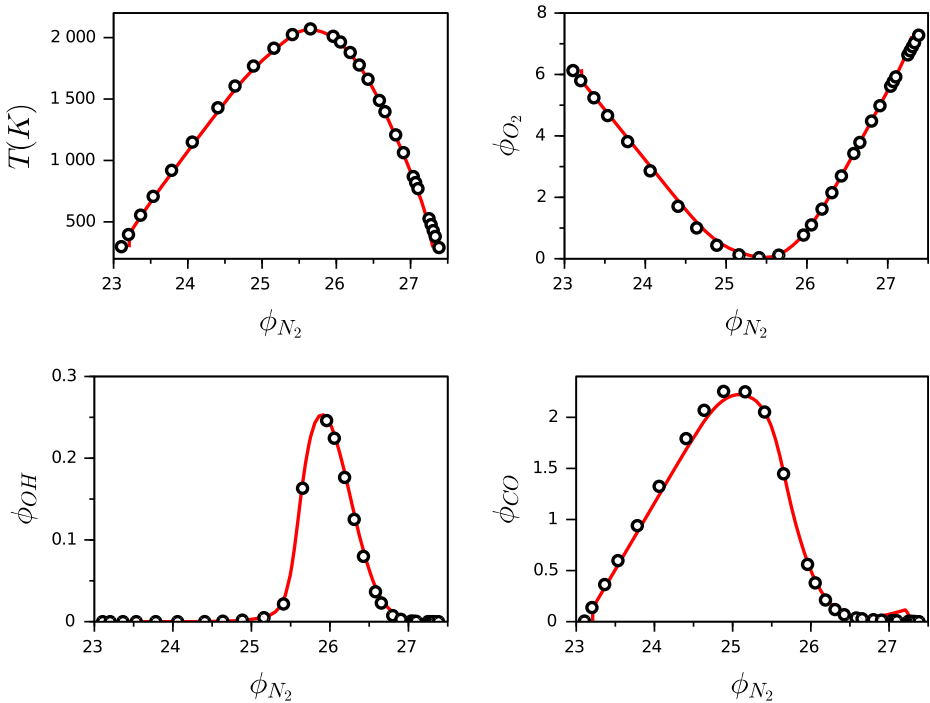


**Fig. 4** Comparison of temperature and specific mole fractions  $\phi$  of  $O_2$ ,  $OH$  and  $CO$  over the specific mole fraction of  $N_2$  for the counterflow non-premixed laminar flame ( $\phi_i = w_i/W_i$ , where  $w_i$  is the mass fraction and  $W_i$  the molar mass of species  $i$ ). Circles: detailed chemistry; line: reduced chemistry

## 5.2 Laminar case

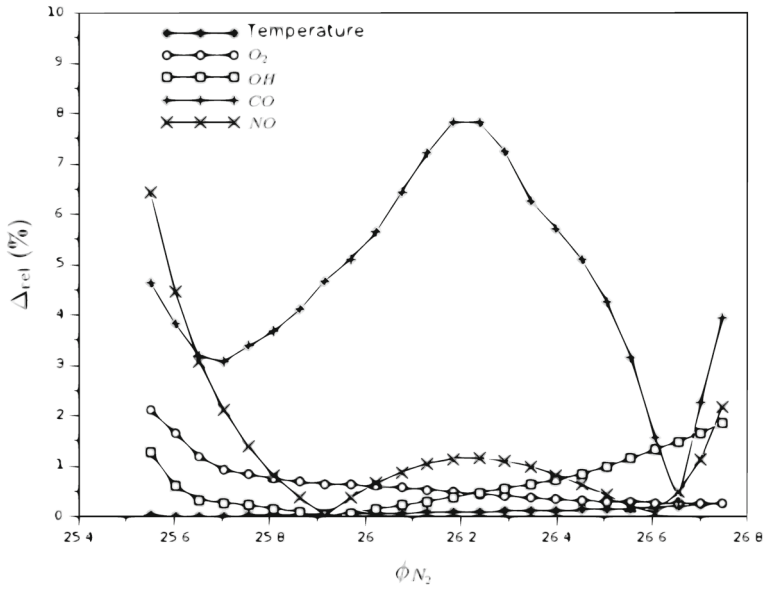
Validation of the 2D REDIM reduced model is performed using a numerical simulation of a laminar counter-flow non-premixed flame, where the results are compared with detailed chemistry. Figure 4 shows the temperature and the specific mole fractions of  $O_2$ ,  $OH$  and  $CO$ , plotted against the specific mole fraction of  $N_2$ . It can be observed that, even using a simplified gradient guess, the results from constructed REDIM agree very well with the simulation based on detailed chemistry for all four quantities.

The deviations between reduced and detailed model are quantified in Fig. 5 where the error deviations are calculated with

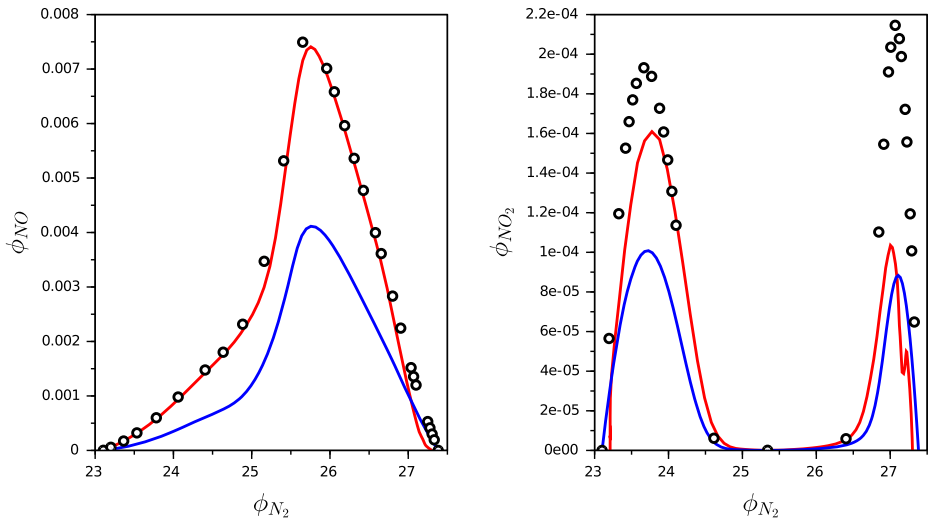
$$\Delta_{\text{rel}} = 100 \times \left| \frac{f_{\text{detailed}} - f_{\text{reduced}}}{f_{\text{detailed}}} \right| \quad (14)$$

where  $f$  is the variable of interest. The profiles are calculated in the reaction zone of the flame and shows that the global maximum error is less than 8%, while errors for temperature and mass fractions of  $O_2$  and  $OH$  are close to 1%.

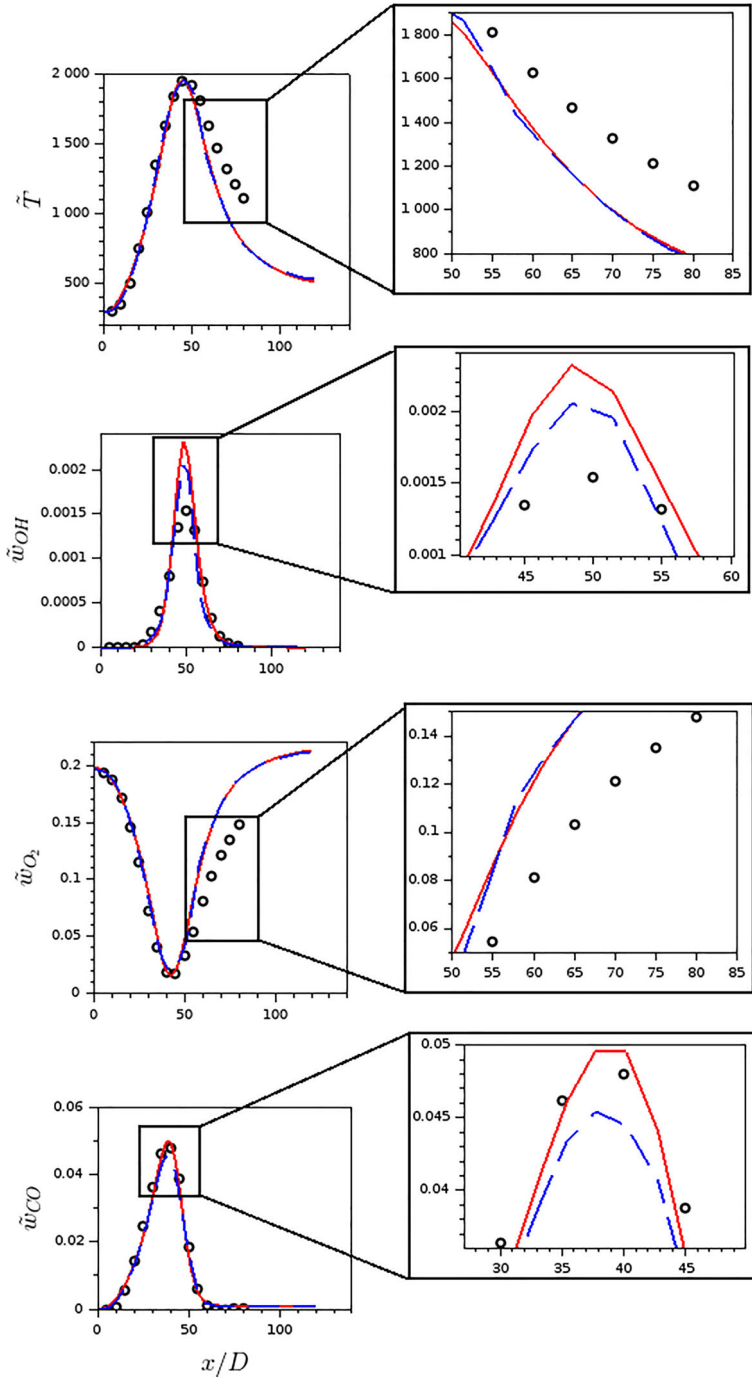
Figure 6 shows the specific mole fraction of  $NO$  and  $NO_2$  over  $N_2$  for the laminar counter-flow non-premixed flame (circle is detailed chemistry and red line the REDIM predictions). Both values show good agreement and  $NO$  profiles errors are below 4% (see



**Fig. 5** Relative error predictions for laminar counter-flow non-premixed flame. Results are plotted only for the reaction zone of the flame



**Fig. 6** Comparison of specific mole fractions  $\phi$  of NO and NO<sub>2</sub> over the specific mole fraction of N<sub>2</sub> for the counterflow non-premixed laminar flame. Circles: detailed chemistry (GRI 3.0); red line: reduced chemistry; blue dashed line: detailed chemistry (GRI 2.11)



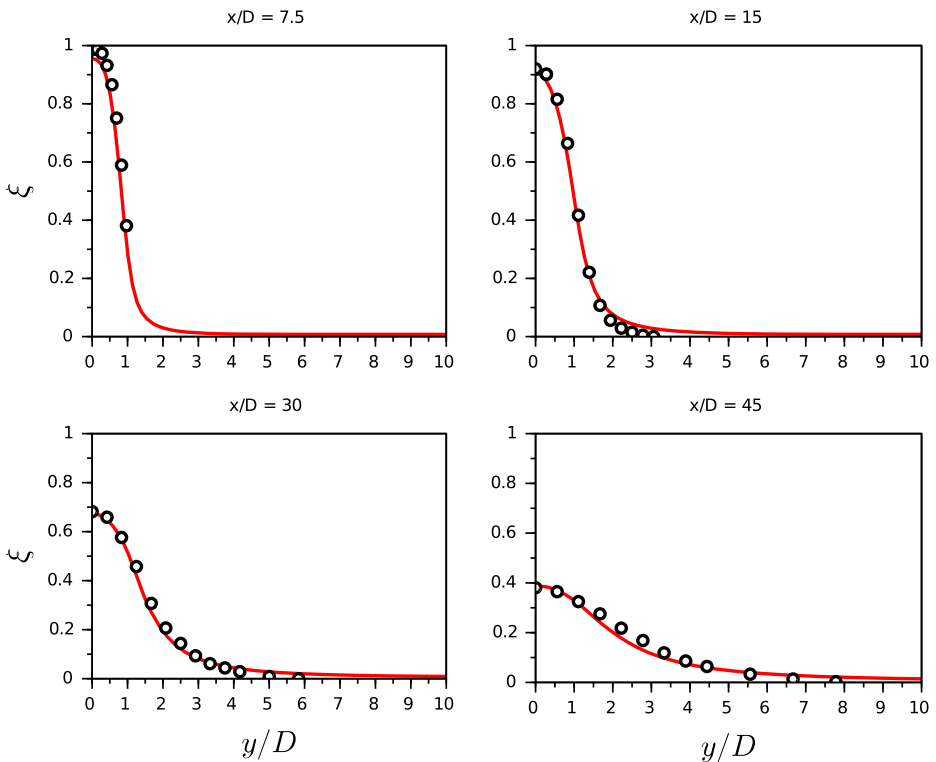
**Fig. 7** Favre-averaged profiles of temperature,  $w_{O_2}$ ,  $w_{OH}$  and  $w_{CO}$  for the turbulent flame Sandia D along the center line of the main jet. Details show the discrepancies between models. Circles: experiment [43]; red lines: simulation with simplified REDIM; blue dashed lines: simulation with detailed REDIM

Fig. 5), while the peak values for  $\text{NO}_2$  in both lean and rich regions of the flame are under-predicted by the REDIM. Nevertheless, to show that this error is reasonable, we also show in Fig. 6 the results from a detailed simulation using GRI 2.11 mechanism [48] (blue dashed line), which shows that, for the detailed chemistry comparison, there are larger discrepancies between both full models, and the REDIM solution is in between this deviation.

Thus, not only the fast but the slow processes represented by those pollutants can be described with the simplified gradient estimation for the REDIM methodology.

### 5.3 Turbulent cases

The numerical simulation of the turbulent flame using the hybrid strategy RANS/transported-PDF is compared with the experimental data available for the Sandia flame D [43]. The mixture fraction is obtained using the Bilger expression, the same way it was done for the experiments. A numerical simulation performed using a REDIM constructed with a more complex gradient guess, consisting of several flamelets with different strain rates, is also used for comparison. In what follows, this configuration will be referred as detailed REDIM.



**Fig. 8** Mean radial profiles for mixture fraction at four different locations of the flame, compared with experimental data, for Sandia flame D. Circles: experiment [43]; red lines: simulation with simplified REDIM

Figure 7 shows the profiles of temperature and mass fractions of  $O_2$ , OH and CO along the center line of the jet ( $r = 0$ ), compared with the experimental data [43] and detailed REDIM. The simulation results shows that the simplified approach for the REDIM has the same global behaviour as the experiments. There is a very good accuracy from the burner exit until approximately  $x/D = 60$  while for  $x/D > 60$ , the temperature and the mass fractions of OH and  $O_2$  show larger deviations from the experimental results, which are also observed for the detailed REDIM results (see zoom details in Fig. 7). Although considerable, the discrepancies are related to the mixing model used in the simulations, since it was already shown that using a different mixing model with optimal parameters can correct this

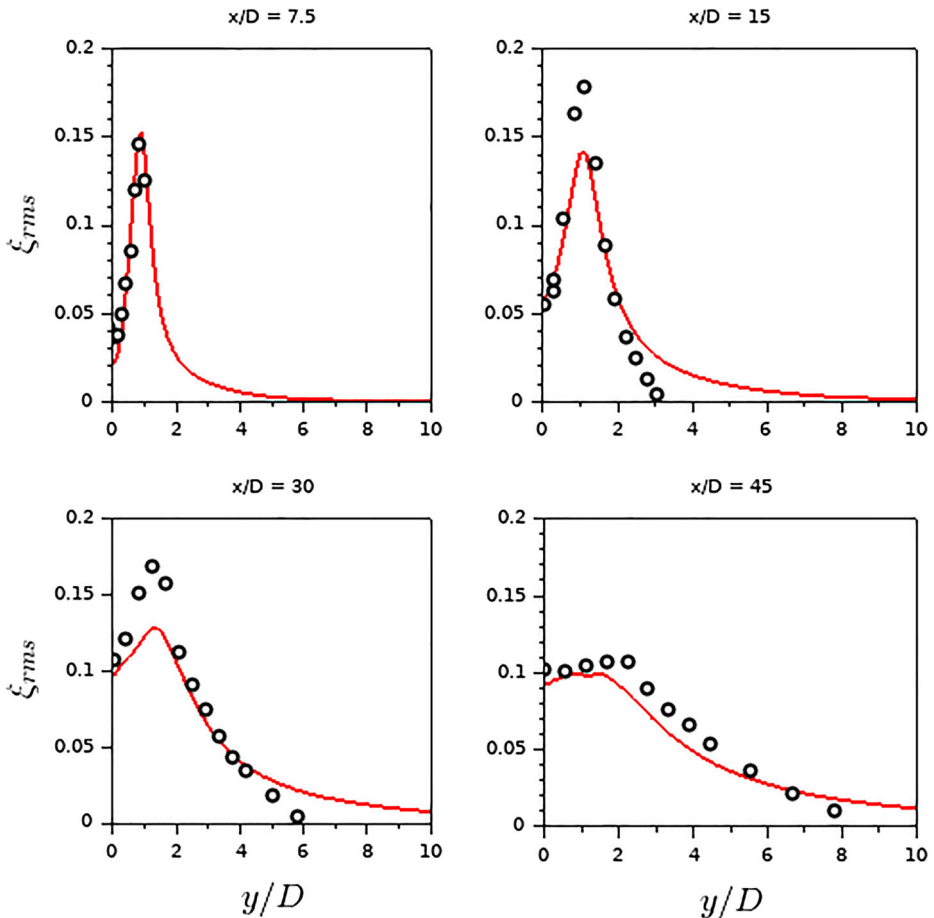


**Fig. 9** Mean radial profiles for rms of mixture fraction at four different locations of the flame, compared with experimental data, for Sandia flame D. Circles: experiment [43]; red lines: simulation with simplified REDIM

difference [40]. However, this would lead to an increase in the computational cost and, as this work aims to investigate the ability of the REDIM simplified configuration, we choose to use the MCM method.

Figures 8 and 9 present the radial profile for the mean and root mean square (rms) of mixture fraction for four different locations of the flame along the mixture fraction space, compared with the experimental data. The simulation results agree well with the experiment data for all locations. Some deviation is seen for the rms of mixture fraction at  $x/D = 15$  and  $x/D = 30$ , where a under-prediction is observed. This deviation is also associated with the mixing model [40].

Figures 10, 11 and 12 display the conditional means of temperature and mass fractions of CO and OH over the mixture fraction at four different locations of the flame, compared with experimental data. The calculated temperature profiles (Fig. 10) reproduce very well the experiment, with almost no deviation from the experimental data at the four locations of the flame.

The conditional mass fraction of CO (Fig. 11) shows some deviations far from the burner nozzle, in the positions  $x/D = 30$  and  $x/D = 45$ , while the mass fractions of OH (Fig. 12)

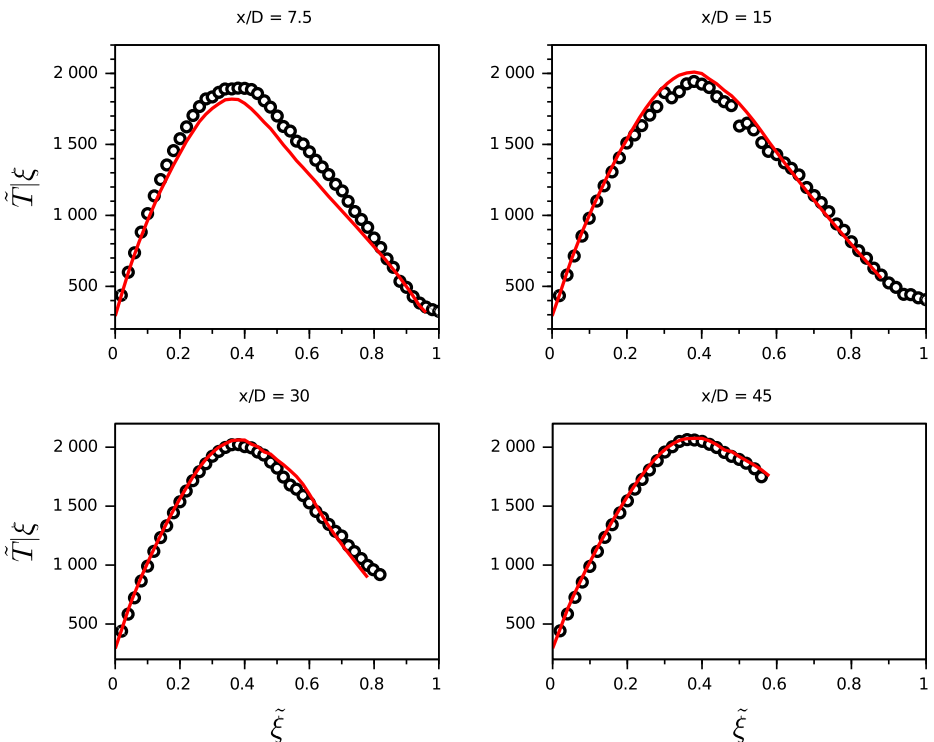


**Fig. 10** Conditional of temperature over the mixture fraction at four different locations of the flame, compared with experimental data, for Sandia flame D. Circles: experiment [43]; red lines: simulation with simplified REDIM

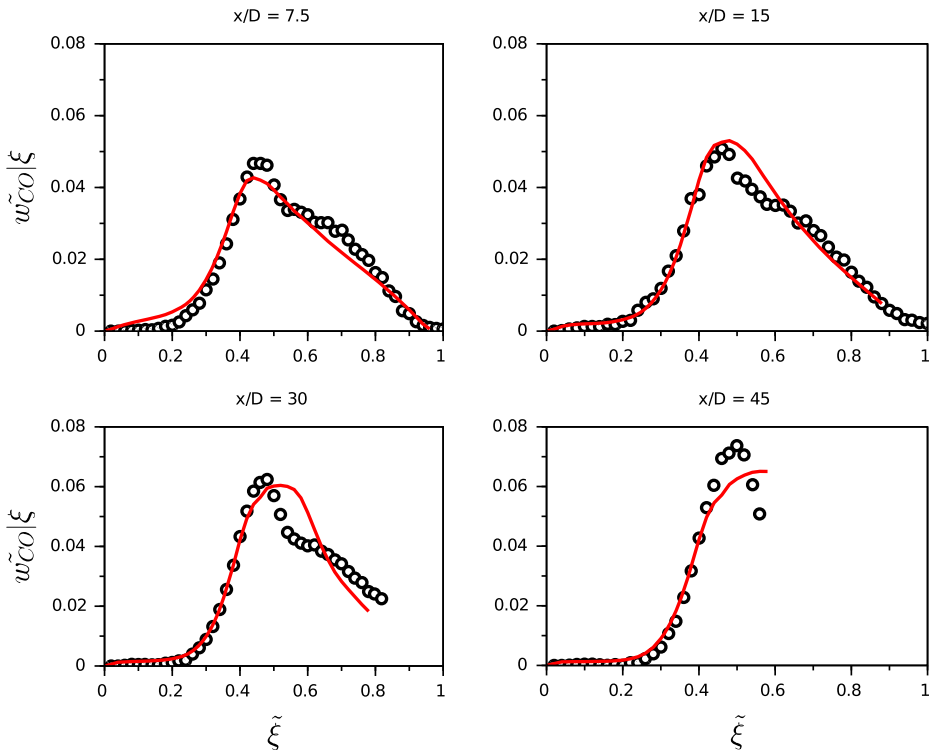


**Fig. 11** Conditional mass fraction of CO over the mixture fraction at four different locations of the flame, compared with experimental data, for Sandia flame D. Circles: experiment [43]; red lines: simulation with simplified REDIM

are over-predicted for  $x/D = 15$ ,  $x/D = 30$  and  $x/D = 45$ . These small differences between the experiment and the numerical simulation are not large, and are possibly associated with the used gradient assumption. Another possibility for these deviations are due to the turbulence model, and better results could be achieved with a more accurate model, such as large eddy simulation (LES) [49].

We also present here the ability of the simplified configuration for the REDIM to reproduce the Sandia flame E, which presents a moderate degree of local extinction. Figures 13, 14 and 15 show the conditional means of temperature, and mass fractions of CO and OH over the mixture fraction at four different locations of the flames. The temperature profile for  $x/D = 15$  shows an over-prediction, which can be justified by the mixing model that is used. Conditional means mass fractions of CO and OH (Figs. 14 and 15) presents over-prediction for almost all locations of the flame, except for the mass fraction of CO at  $x/D = 45$ . The same behaviour can be seen when a detailed REDIM configuration for the gradient estimation (consisting of several flamelets with different strain rates) is used, as show in [50–52], and thus, is believed that the over/under-prediction for CO and OH can be related either to the detailed mechanism or the mixing model.



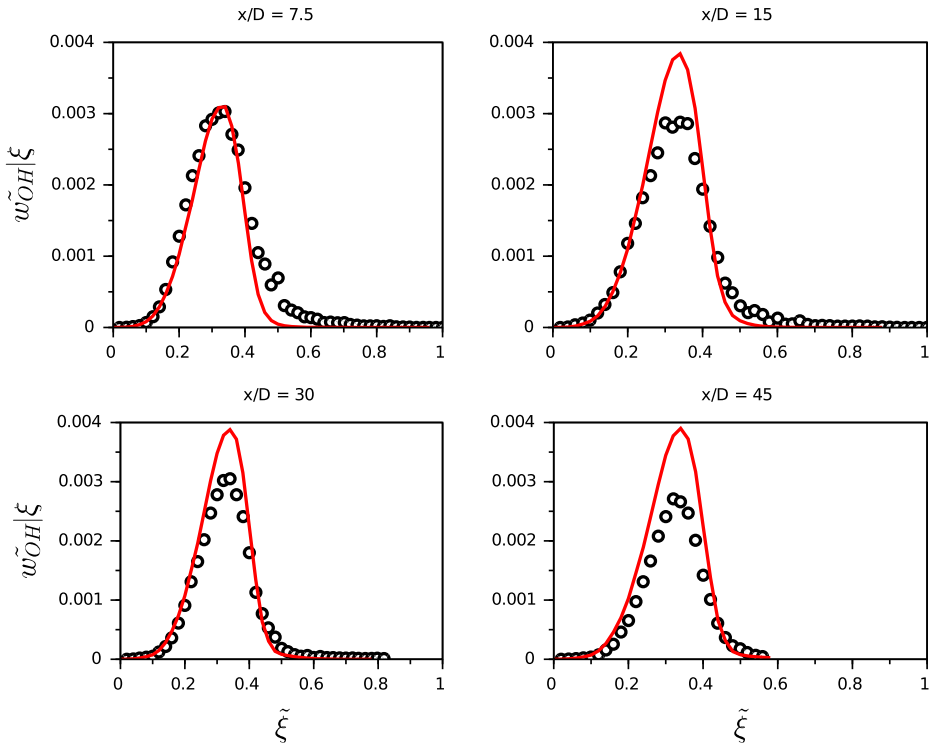


**Fig. 12** Conditional mass fraction of OH over the mixture fraction at four different locations of the flame, compared with experimental data, for Sandia flame D. Circles: experiment [43]; red lines: simulation with simplified REDIM

### 5.4 Computational performance

We show in Fig. 16 the CPU costs for laminar flame simulations using the simplified REDIM compared with a full detailed mechanism simulation. The values of Fig. 16 are normalized by the value of full mechanism. One can see that the CPU cost is considerably decreased in the flames simulations and, contrasted with using the full kinetic mechanism, simulation with simplified REDIM yields a reduction in computational time of 91%. This substantial decrease is associated with the fact that the REDIM is stored within an orthogonal and equidistant mesh, which is optimized for an adequate linear interpolation, and a point-by-point search is not required [27].

For the turbulent flame simulations, we do not have a comparison with simulations using the detailed mechanism, because these are computationally expensive. Nevertheless, if we compare the CPU cost of our simplified REDIM with the detailed REDIM (i.e., the gradient guess is obtained from several flamelets with different strain rates), the decrease of the computational time is in the order of 25% for Sandia flame D and 21% for Sandia E. Moreover, simplified configuration has the computational advantage of only needing three

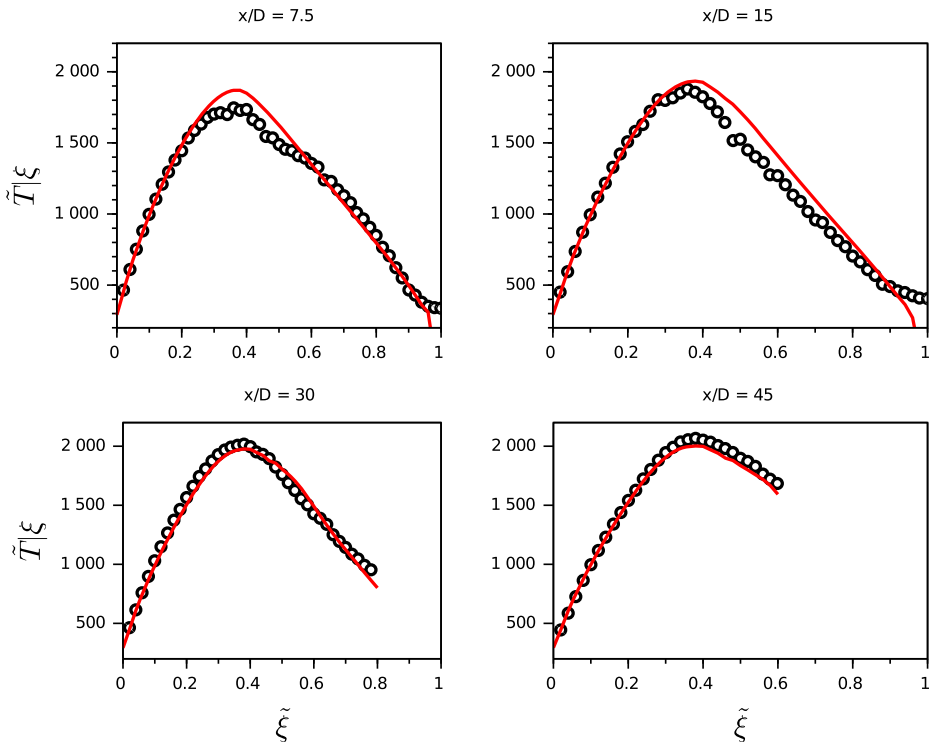


**Fig. 13** Conditional of temperature over the mixture fraction at four different locations of the flame, compared with experimental data, for Sandia flame E. Circles: experiment [43]; red lines: simulation with simplified REDIM

detailed flamelets simulations to construct the initial profile for integration of Eq. 7, which not only reduces CPU cost but also the size of the lookup table that will be used in the search and retrieve algorithm.

The results presented above may be subject to the influence of different values chosen for the strain rate  $a$  considered in the flamelet solution with low stretch rate in the simplified configuration. As the REDIM equation depends on the gradient of the local coordinates, and since the strain rate depends on the velocity gradients, the higher the value of  $a$ , more the flame is perturbed by the transport processes [30], which can lead to, e.g., earlier/later extinction. In the present work, we choose  $a = 200$  1/s, since for this value the flame is considered stable and far from any critical point.

In this section, we showed that even a simplified configuration of the initial guess to construct REDIM is able to describe chemistry in a turbulent flame that has a small and a moderate degree of local extinction. Since the gradients are obtained from detailed numerical simulation of flamelets with different stretch rates, the obtainment of a initial profile can be computationally demanding. Thus, the simplified configuration is a good strategy to overcome this problem.

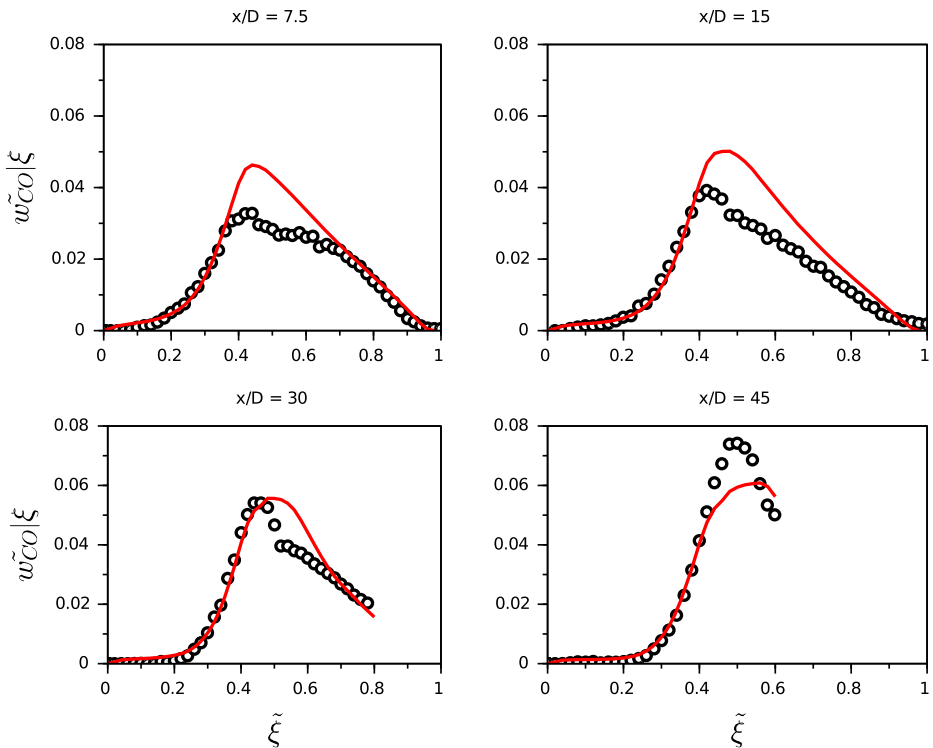


**Fig. 14** Conditional mass fraction of CO over the mixture fraction at four different locations of the flame, compared with experimental data, for Sandia flame E. Circles: experiment [43]; red lines: simulation with simplified REDIM

## 6 Conclusions

The use of REDIM is an efficient tool to solve the complex chemistry modeling but, depending on the size of the full model, the computational cost can still be high to generate the gradient estimation and initial profile, as well as to solve the REDIM-equation. Therefore, the strategy developed in this work enables to have a simplified generation of the initial profile (with less information about the full model) which leads to a faster integration of the REDIM equation and also a reduction of the size of the data files that will be used when the method is coupled with CFD simulation.

We showed that the simple gradient estimation used for the REDIM model reduction technique can be used to simulate a methane/air turbulent piloted flame, with a small and moderate degree of local extinction. Validation of the proposed strategy is performed for laminar counter-flow non-premixed flames by comparison of detailed and reduced models and computational results for a turbulent flame are compared to experimental results. It is shown that the simplified gradient estimation can predict with accuracy the thermodynamic parameters and species profiles, which shows the efficiency of the proposed strategy of the REDIM in modeling reactive flows.

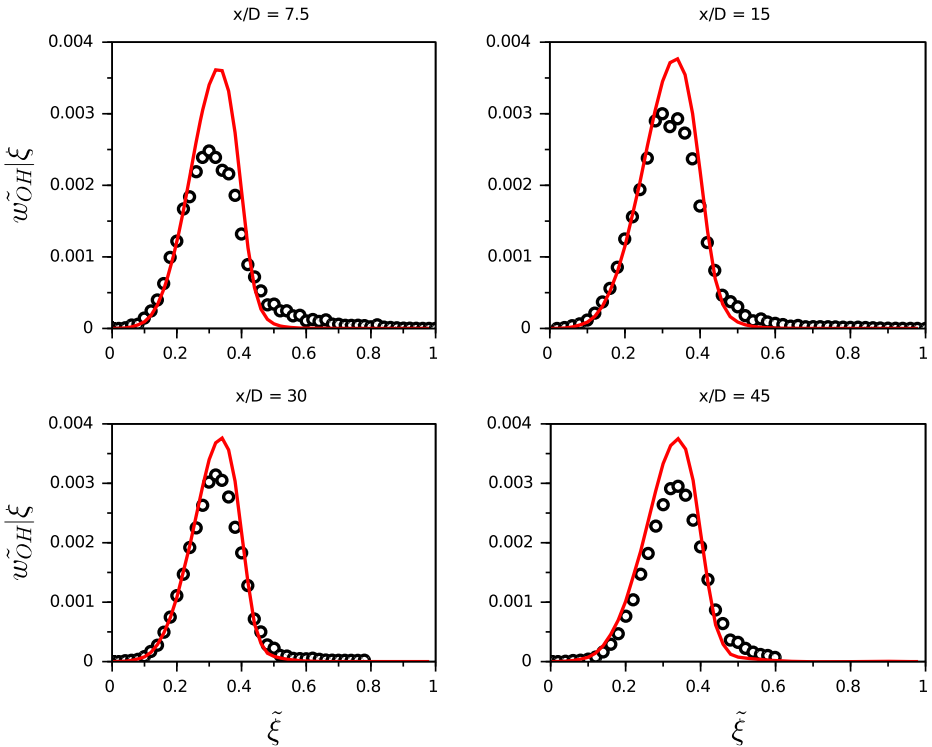


**Fig. 15** Conditional mass fraction of OH over the mixture fraction at four different locations of the flame, compared with experimental data, for Sandia flame E. Circles: experiment [43]; red lines: simulation with simplified REDIM

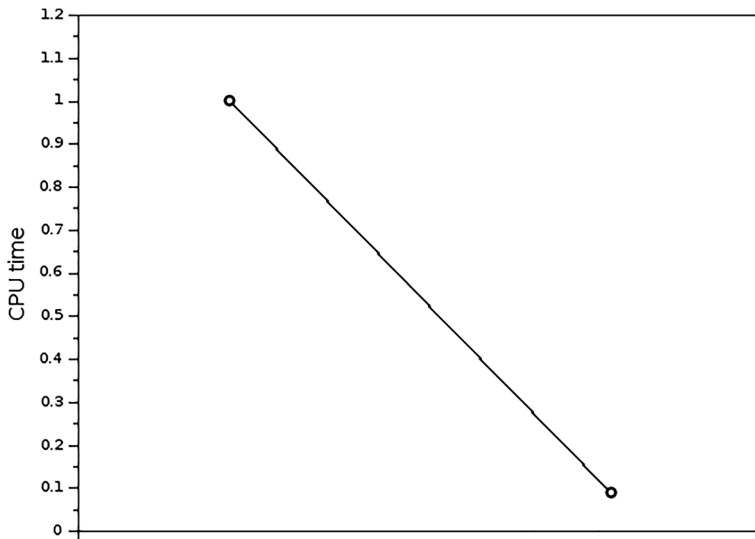


**Fig. 16** CPU cost for laminar flame simulation, normalized by the detailed mechanism simulation time

**Acknowledgements** Financial support by the German Research Foundation (DFG) within the project SFB/TR150 is gratefully acknowledged. F. Minuzzi was supported by CAPES - Brazil, during his stay in Germany, under the grant N° 88881.132868/2016-01.

## Compliance with Ethical Standards

**Conflict of interests** The authors declare that they have no conflict of interest.

## References

1. Vervisch, L.: Numerical modeling of nonpremixed turbulent combustion. Institut National des Sciences Appliquees de Rouen (1999)
2. Kuo, K., Acharya, R.: Fundamentals of Turbulent and Multi-Phase Combustion. Wiley, New York (2012)
3. Peters, N.: Turbulent Combustion. Cambridge University Press, Cambridge (2000)
4. Pope, S.: Turbulent Flows. IOP Publishing, Bristol (2001)
5. Warnatz, J., Maas, U., Dibble, R. Combustion: Physical and Chemical Fundamentals, Modeling and Simulation, Experiments, Pollutant Formation, 4th edn. Springer, Berlin (2006)
6. Poinso, T., Veynante, D. Theoretical and Numerical Combustion, 3rd edn. Inc, RT Edwards (2011)
7. Echehki, T., Mastorakos, E.: Turbulent Combustion Modeling: Advances, New Trends and Perspectives, vol. 95. Springer, Berlin (2010)
8. Pitsch, H.: Large-eddy simulation of turbulent combustion. *Annu. Rev. Fluid Mech.* **38**, 453–482 (2006)
9. Spalding, D.: Mixing and chemical reaction in steady confined turbulent flames. In: Symposium (International) on Combustion, vol. 13, pp. 649–657. Elsevier (1971)
10. Pope, S.: PDF methods for turbulent reactive flows. *Prog. Energy Combust. Sci.* **11**(2), 119–192 (1985)
11. Haworth, D.: Progress in probability density function methods for turbulent reacting flows. *Prog. Energy Combust. Sci.* **36**(2), 168–259 (2010)
12. Turányi, T., Tomlin, A.S.: Analysis of kinetic reaction mechanisms. Springer, Berlin (2014)
13. Lu, T., Law, C.K.: On the applicability of directed relation graphs to the reduction of reaction mechanisms. *Combust. Flame* **146**(3), 472–483 (2006)
14. Lu, T., Law, C.K.: A directed relation graph method for mechanism reduction. *Proc. Combust. Inst.* **30**(1), 1333–1341 (2005)
15. Pepiot-Desjardins, P., Pitsch, H.: An efficient error-propagation-based reduction method for large chemical kinetic mechanisms. *Combust. Flame* **154**(1), 67–81 (2008)
16. Bodenstein, M.: Eine theorie der photochemischen reaktionsgeschwindigkeiten. *Zeitschrift für Physikalische Chemie* **85**(1), 329–397 (1913)
17. Maas, U., Pope, S.: Simplifying chemical kinetics: intrinsic low-dimensional manifolds in composition space. *Combust. Flame* **88**(3), 239–264 (1992)
18. Gicquel, O., Darabiha, N., Thévenin, D.: Laminar premixed hydrogen/air counterflow flame simulations using flame prolongation of ILDM with differential diffusion. *Proc. Combust. Inst.* **28**(2), 1901–1908 (2000)
19. Lam, S.: Using CSP to understand complex chemical kinetics. *Combust. Sci. Technol.* **89**(5-6), 375–404 (1993)
20. Williams, F.: Recent advances in theoretical descriptions of turbulent diffusion flames. In: *Turbulent Mixing in Nonreactive and Reactive Flows*, pp. 189–208. Springer (1975)
21. Pierce, C.D., Moin, P.: Progress-variable approach for large-eddy simulation of non-premixed turbulent combustion. *J. Fluid Mech.* **504**, 73–97 (2004)
22. Oijen, J.V., Goey, L.D.: Modelling of premixed laminar flames using flamelet-generated manifolds. *Combust. Sci. Technol.* **161**(1), 113–137 (2000)
23. Goussis, D.A., Maas, U.: Model reduction for combustion chemistry. In: *Turbulent Combustion Modeling*, pp. 193–220. Springer (2011)
24. Griffiths, J.: Reduced kinetic models and their application to practical combustion systems. *Prog. Energy Combust. Sci.* **21**(1), 25–107 (1995)
25. Løvås, T.: Model reduction techniques for chemical mechanisms. INTECH Open Access Publisher (2012)
26. Tomlin, A.S., Turányi, T., Pilling, M.J.: Mathematical tools for the construction, investigation and reduction of combustion mechanisms. *Comprehensive Chemical Kinetics* **35**, 293–437 (1997)

27. Bykov, V., Maas, U.: The extension of the ILDM concept to reaction–diffusion manifolds. *Combust. Theor. Model.* **11**(6), 839–862 (2007)
28. Bykov, V., Neagos, A., Maas, U.: On transient behavior of non-premixed counterflow diffusion flames within the REDIM based model reduction concept. *Proc. Combust. Inst.* **34**(1), 197–203 (2013)
29. Bykov, V., Maas, U.: Problem adapted reduced models based on reaction–diffusion manifolds (REDIMs). *Proc. Combust. Inst.* **32**(1), 561–568 (2009)
30. Fischer, S., Markus, D., Ghorbani, A., Maas, U.: PDF simulations of the ignition of hydrogen/air, ethylene/air and propane/air mixtures by hot transient jets. *Zeitschrift für Physikalische Chemie* **231**(10), 1773–1796 (2017)
31. Wang, P., Platova, N., Fröhlich, J., Maas, U.: Large eddy simulation of the PRECCINSTA burner. *Int. J. Heat Mass Transf.* **70**, 486–495 (2014)
32. Wang, P., Zieker, F., Schießl, R., Platova, N., Fröhlich, J., Maas, U.: Large eddy simulations and experimental studies of turbulent premixed combustion near extinction. *Proc. Combust. Inst.* **34**(1), 1269–1280 (2013)
33. Steinhilber, G., Bykov, V., Maas, U.: REDIM reduced modeling of flame-wall-interactions: quenching of a premixed methane/air flame at a cold inert wall. *Proc. Combust. Inst.* **36**(1), 655–661 (2017)
34. Schießl, R., Bykov, V., Maas, U., Abdelsamie, A., Thévenin, D.: Implementing multi-directional molecular diffusion terms into reaction diffusion manifolds (REDIMs). *Proc. Combust. Inst.* **36**(1), 673–679 (2017)
35. Benzinger, M.S., Schießl, R., Maas, U.: A versatile coupled progress variable/REDIM, model for auto-ignition and combustion. *Proc. Combust. Inst.* **36**(3), 3613–3621 (2017)
36. Pope, S.: A Monte Carlo method for the PDF equations of turbulent reactive flow. *Progress Combust. Energy Sci.* **25** (1981)
37. Yu, C., Minuzzi, F., Maas, U.: Numerical simulation of turbulent flames based on a hybrid RANS/Transported-PDF method and REDIM method. *Eurasian Chem. Technol. J.* **20**(1), 23–31 (2018)
38. Jenny, P., Pope, S., Muradoglu, M., Caughey, D.: A hybrid algorithm for the joint PDF equation of turbulent reactive flows. *J. Comput. Phys.* **166**(2), 218–252 (2001)
39. Curl, R.: Dispersed phase mixing: i. theory and effects in simple reactors. *AIChE J.* **9**(2), 175–181 (1963)
40. Cao, R.R., Wang, H., Pope, S.B.: The effect of mixing models in PDF calculations of piloted jet flames. *Proc. Combust. Inst.* **31**(1), 1543–1550 (2007)
41. Rembold, B., Jenny, P.: A multiblock joint PDF finite-volume hybrid algorithm for the computation of turbulent flows in complex geometries. *J. Comput. Phys.* **220**(1), 59–87 (2006)
42. Muradoglu, M., Jenny, P., Pope, S.B., Caughey, D.A.: A consistent hybrid finite-volume/particle method for the PDF equations of turbulent reactive flows. *J. Comput. Phys.* **154**(2), 342–371 (1999)
43. International workshop on measurement and computation of turbulent nonpremixed flames. [Online]. Available: <http://www.sandia.gov/TNF/abstract.html>
44. Barlow, R., Frank, J.: Effects of turbulence on species mass fractions in methane/air jet flames. In: *Symposium (International) on Combustion*, vol. 27, pp. 1087–1095. Elsevier (1998)
45. Magagnato, F.: SPARC: structured parallel research code. *Task Quarterly* **2**(2), 215–270 (1998)
46. Maas, U.: *Mathematische Modellierung Instationärer Verbrennungsprozesse Unter Verwendung Detaillierter Reaktionsmechanismen*. Ph.D. Thesis, Ruprecht-Karls-Universität, Heidelberg, Germany (1988)
47. Smith, G., Golden, D., Frenklach, M., Moriarty, N., Eiteneer, B., Goldenberg, M., Bowman, C., Hanson, R., Song, S., Gardiner, W., Lissianski, V., Qin, Z.: Gri-mech 3.0. GRI-Mech Home Page, [http://www.me.berkeley.edu/gri\\_mech/](http://www.me.berkeley.edu/gri_mech/) (2011)
48. Bowman, C., Hanson, R., Davidson, W., Gardiner, W., Lissianski, V., Smith, G., Golden, D., Frenklach, M., Goldenberg, M.: Gri-mech 2.11. GRI-Mech Home Page, [http://www.me.berkeley.edu/gri\\_mech/](http://www.me.berkeley.edu/gri_mech/) (1995)
49. Ge, Y., Cleary, M., Klimenko, A.: A comparative study of Sandia flame series (D–F) using sparse-lagrangian MMC modelling. *Proc. Combust. Inst.* **34**(1), 1325–1332 (2013)
50. Cao, R.R., Pope, S.B.: The influence of chemical mechanisms on PDF calculations of nonpremixed piloted jet flames. *Combust. Flame* **143**(4), 450–470 (2005)
51. Xu, J., Pope, S.B.: PDF calculations of turbulent nonpremixed flames with local extinction. *Combust. Flame* **123**(3), 281–307 (2000)
52. Yu, C., Bykov, V., Maas, U.: Coupling of simplified chemistry with mixing processes in PDF simulations of turbulent flames. *Proc. Combust. Inst.* **37**(2), 2183–2190 (2019)